A four-point molecular handover during Okazaki maturation

Botto, M.M.; Borsellini, A.; Lamers, M.H.

nature structural & molecular biology

Article

https://doi.org/10.1038/s41594-023-01071-y

A four-point molecular handover during Okazaki maturation

Received: 30 July 2022

Accepted: 17 July 2023

Published online: 24 August 2023

Check for updates

Margherita M. Botto[1,2], Alessandro Borsellini[1,3] & Meindert H. Lamers[1]

DNA replication introduces thousands of RNA primers into the lagging strand that need to be removed for replication to be completed. In *Escherichia coli* when the replicative DNA polymerase Pol IIIα terminates at a previously synthesized RNA primer, DNA Pol I takes over and continues DNA synthesis while displacing the downstream RNA primer. The displaced primer is subsequently excised by an endonuclease, followed by the sealing of the nick by a DNA ligase. Yet how the sequential actions of Pol IIIα, Pol I polymerase, Pol I endonuclease and DNA ligase are coordinated is poorly defined. Here we show that each enzymatic activity prepares the DNA substrate for the next activity, creating an efficient four-point molecular handover. The cryogenic-electron microscopy structure of Pol I bound to a DNA substrate with both an upstream and downstream primer reveals how it displaces the primer in a manner analogous to the monomeric helicases. Moreover, we find that in addition to its flap-directed nuclease activity, the endonuclease domain of Pol I also specifically cuts at the RNA–DNA junction, thus marking the end of the RNA primer and creating a 5′ end that is a suitable substrate for the ligase activity of LigA once all RNA has been removed.

In *Escherichia coli*, DNA replication is performed by the DNA polymerase III holoenzyme at speeds of up to 1,000 nucleotides (nt) per second[1,2] and 100,000 base pairs (bp) per binding event[3]. DNA replication occurs asymmetrically, where the leading strand is synthesized in a continuous fashion while the lagging strand is synthesized in 500–1,000 bp Okazaki fragments[4,5] resulting in 9,000 fragments for the 4.6 million bp *E. coli* genome[6]. As the replicative DNA polymerase, the α subunit of the DNA polymerase III holoenzyme (Pol IIIα) cannot start DNA synthesis de novo, each Okazaki fragment is initiated by a 10–15 nt RNA primer that is synthesized by the DNA primase DnaG (refs. 7,8). To complete DNA replication, these thousands of RNA primers are removed from the DNA by the concerted action of Pol IIIα, DNA polymerase I (Pol I), the endonuclease domain of Pol I and a DNA ligase.

The roles of the individual proteins and subunits have been well described[9]. The bulk of the DNA is synthesized by Pol IIIα, a fast and highly processive enzyme[10,11] that disengages from the DNA when it encounters a downstream RNA primer[12]. Pol I that is capable of strand displacement of the downstream RNA primer then continues DNA synthesis[13,14]. The displaced RNA primer is then removed by the N-terminal domain of Pol I that is a flap-directed 5′–3′ exo- or endonuclease[15–18], followed by sealing of the nick by a DNA ligase[19,20].

Several fundamental questions remain about how the removal of the RNA primer is orchestrated. (1) How is Pol I able to continue DNA synthesis where Pol IIIα comes to a halt? (2) How does Pol I detect the end of the RNA primer? (3) How is the endonuclease activated to cut the displaced RNA flap? (4) What prevents the ligase from ligating the DNA to the RNA primer? And, finally, (5) how are these sequential activities organized in time and prevented from counteracting each other's activities?

Here we present the structure of Pol I engaged with both an upstream (extended) primer and a downstream (displaced) primer. This structure reveals how Pol I acts in a manner analogous to monomeric

[1]Department of Cell and Chemical Biology, Leiden University Medical Center (LUMC), Leiden, the Netherlands. [2]Present address: Department of Molecular and Cellular Biology, Geneva University, Geneva, Switzerland. [3]Present address: Department of Structural Biology, Human Technopole, Milan, Italy. e-mail: m.h.lamers@lumc.nl

https://doi.org/10.1038/s41594-023-01071-y

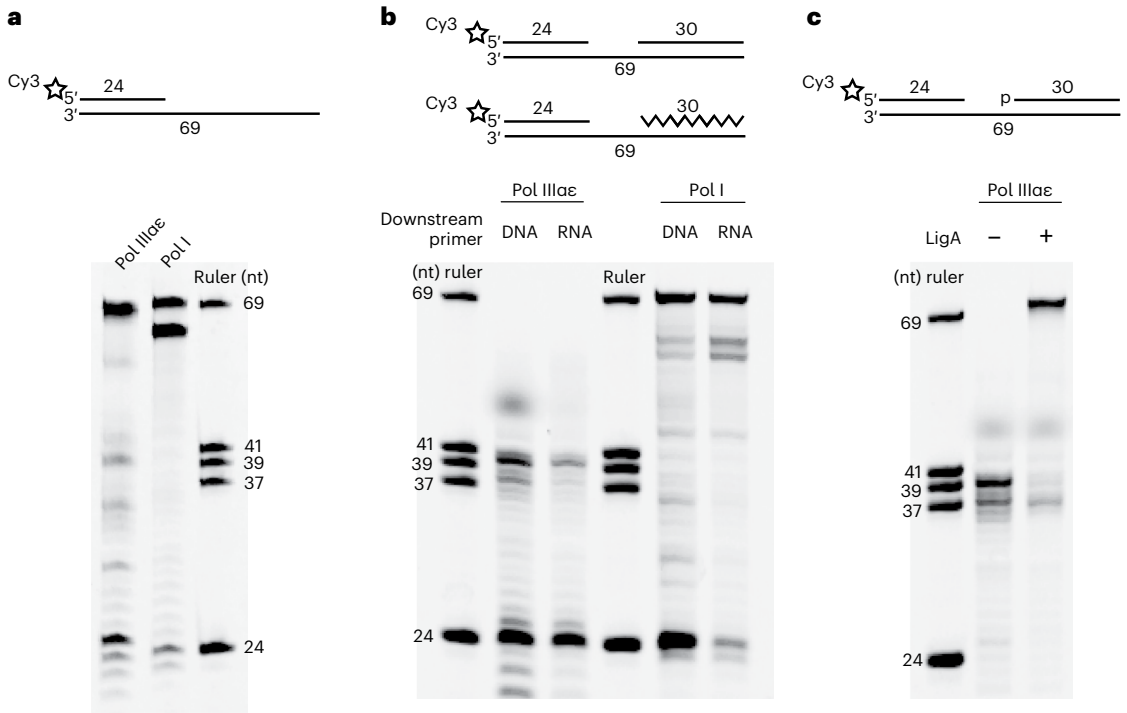

Fig. 1 | Comparison of Pol IIIαε and Pol I primer extension activity. a, DNA synthesis of Pol IIIαε and Pol I on a 69 nt template strand with a single upstream primer. The right lane (marked 'ruler') shows DNA substrates of different lengths as indicated. **b**, DNA synthesis of Pol IIIαε and Pol I on the same substrate as **a** complemented with a DNA or RNA downstream primer. The zig-zag line in the diagram above the gel indicates the RNA primer. **c**, DNA ligase activity by LigA after primer extension between the upstream and downstream primer by Pol IIIαε. The downstream primer contains a 5′ phosphate group needed for ligase activity. All the reactions were performed in presence of the 100 nM β clamp and 100 nM Pol I or Pol IIIαε.

helicases[21,22], where the fingers domain of Pol I acts like a strand separating pin, while the primer extension of Pol I drives DNA translocation, analogous to the ATPase domains of the monomeric helicases. We furthermore present the biochemical analysis of the sequential activities of the four enzymes involved in the Okazaki maturation. We show that the endonuclease domain of Pol I specifically introduces a nick at the RNA–DNA junction, thus marking the end of the RNA primer. In addition, we show that LigA, the dominant *E. coli* DNA ligase, cannot ligate RNA to DNA, but will act as soon as a DNA–DNA junction is available. The ligation of the two Okazaki fragments results in the eviction of Pol I from the DNA, thus completing the Okazaki fragment maturation.

Hence, our work reveals that the different proteins act as a 'molecular relay race', in which each activity prepares the RNA–DNA substrate for the next enzymatic activity to take over. This way, the removal of the thousands of RNA primers from the lagging strand introduced during DNA replication is an efficient process that ensures that an intact DNA is delivered for the next generation of cells.

Results

Molecular handover between Pol IIIα and Pol I

When Pol IIIα encounters a previously synthesized Okazaki fragment it terminates DNA synthesis[12]. While it can perform modest strand displacement, this activity is 300-fold less favorable than normal DNA synthesis and dependent on a long single-stranded flap coated with single-stranded DNA binding protein[23], which is not a natural substrate that the Pol III holoenzyme encounters during DNA replication. By contrast, Pol I is capable of long-distance strand displacement DNA synthesis[13,14], and will continue DNA synthesis when Pol IIIα dissociates from the DNA. To determine how Pol IIIα and Pol I trade place on the DNA we measured their polymerase activity on a DNA substrate containing an upstream primer (the extended primer) in the absence or presence of an RNA or DNA downstream primer (the displaced primer), separated by a 15-nt gap. For the reaction, the β clamp was added, and Pol IIIα was supplemented with its 3′–5′ proofreading exonuclease ε (creating Pol IIIαε), while Pol I contains its own 3′–5′ proofreading exonuclease domain. In the absence of a displaced primer, both polymerases synthesize to the end of the DNA template (Fig. 1a). Similarly, in the presence of a displaced primer Pol I continues until the end of the template strand (Fig. 1b), in agreement with previous results[13,14,24]. By contrast, Pol IIIαε comes to a halt at the start of the displaced primer, irrespective of the RNA or DNA nature of the primer as was previously shown[12]. To determine whether Pol IIIαε leaves a gap or a nick, we used a displaced DNA primer with a 5′ phosphorylated end that is required for DNA ligase activity and added the *E. coli* DNA ligase LigA after initiation of DNA synthesis (Fig. 1c). In the presence of Pol IIIαε and LigA, most of the extended primer is ligated to the displaced primer to create a fully extended product of 69 nt, indicating that Pol IIIαε can continue DNA synthesis up to the very last nucleotide as was reported previously[25,26]. However, during DNA replication, ligation of the newly synthesized DNA segment and the downstream RNA primer is prevented as the 5′ end of the RNA primer starts with a di- or triphosphate nucleotide[7], which is not a suitable substrate for ligase[27].

Cryo-EM structure of Pol I bound to an Okazaki fragment

To understand how Pol I is able to continue DNA synthesis in the presence of a displaced primer, we determined the cryogenic-electron microscopy (cryo-EM) structure of Pol I bound to a DNA substrate containing both an upstream and downstream primer with a 6-nt single-stranded flap to a resolution of 4.3 Å (Fig. 2, Table 1 and Extended Data Fig. 1). Although full-length Pol I was used (Fig. 2c), no density was observed for the endonuclease domain, indicating that it is flexible in this structure. Next, we used a version of Pol I that lacks the N-terminal endonuclease domain (also known as the Klenow fragment, Pol I^{KL}) to collect a large cryo-EM dataset of more than 11,000 images and more

than 500,000 initial particles. This dataset yielded two structures of Pol I bound to the DNA substrate, to a final resolution of 4.0 and 4.1 Å. The first structure shows Pol I^{KL} with the 3′ terminal base pair of the extended primer in the polymerase active site and the 5′ terminal base pair of the displaced primer stacked against the fingers domain (Fig. 2a). The second structure shows the DNA translated by one nucleotide in the direction of DNA synthesis, with one additional nucleotide separated from the displaced primer (Fig. 2b). Furthermore, the translation of the DNA creates an unpaired nucleotide in the polymerase active site as no dNTPs were added to the sample. The 1 nt translation of the DNA is accompanied by a canonical movement of the O-helix and fingers domain[28–30] that creates an open active site for an incoming nucleotide.

Overall, the closed (nontranslated) and open (translated) structures are very similar, and both show a striking 120° kink of the DNA that places the 3′ end of the extended primer in the polymerase active site while the 5′ end of the displaced primer interacts with the fingers domain. While multiple structures of Pol I bound to only an extended primer exist[31–34], our structure also visualizes the displaced primer. The position of the extended primer is identical to that of the previous structures of Pol I bound to a DNA substrate (Extended Data Fig. 1i), while the position of the displaced primer is in agreement with a recent study where Förster resonance energy transfer was used to predict its location[35]. Our structure reveals the molecular details of the interactions between Pol I and the displaced primer (Fig. 2d), which are best defined in the closed structure. The first base pair of the displaced section interacts with phenylalanine 771 (F771) and arginine 781 (R781) that stack on the template and primer base, respectively. Arginine 841 (R841), positioned under the template strand, acts as a pivot point over which the DNA is bent. F771 and R841 were previously shown to be important for the strand displacement activity of Pol I (ref. 14). The displaced section of the DNA has only limited contacts with the protein, in contrast to the extended section of the DNA (Fig. 2e). Concordantly, the cryo-EM map for the displaced section of the DNA is poorly resolved and only nine of the 18 base pairs can be placed (Fig. 2a,f, left panel). By contrast, the cryo-EM map for the extended DNA section is well resolved in which all 18 base pairs can be placed. On translocation of the DNA in the open structure, the displaced DNA section shows an even weaker cryo-EM map, indicating even less interaction with the displaced DNA section (Fig. 2b,f, right panel, and Supplementary Video 1).

In the polymerase active site of the closed structure, the 3′ terminal base pair is stacked against the O-helix (Fig. 2g), while in the open structure the DNA and O-helix have moved in opposite directions (Fig. 2h). During this movement, two aromatic residues, phenylalanine 762 and tyrosine 766, trade places. In the closed structure, phenylalanine 762 stacks onto the sugar ring of the 3′ terminal nucleotide of the extended strand, while tyrosine 766 is tucked away under the DNA (Fig. 2g). In the open structure, phenylalanine 762 is separated from the 3′ terminal nucleotide by roughly 6 Å, while tyrosine 766 now stacks on the base of the template strand (Fig. 2h). A similar positioning of the two equivalent residues phenylalanine 710 and tyrosine 714 was also observed in *Geobacillus stearothermophilus* Pol I (ref. 30). Due to the 1-nt translation of the template strand, a single unpaired nucleotide is created in the polymerase active site (nucleotide 18 of the template strand) as no dNTPs were added to the sample. Its base pairing partner in the closed structure has now become part of the single-stranded flap and is no longer visible in the cryo-EM map.

The movements described above raise the question as to how the translation is achieved in the absence of dNTPs. Inspection of the polymerase active site reveals a negatively charged patch that could act as a repulsive force to the negatively charged backbone of the DNA (Fig. 2i) and result in the 1 nt translation of the DNA.

A molecular morph between the two structures gives further insight into how the DNA moves through the protein during DNA synthesis (Supplementary Video 2). As the extended strand moves out of the active site, it pulls along the continuous template strand. This, in turn, pulls the displaced strand into the fingers domain, resulting in the displacement of the downstream primer and the lengthening of the single-stranded flap. The translocation of the template strand pulls the next template base into the polymerase active site where it is ready to pair with the next incoming nucleotide.

The mechanism of strand separation in Pol I can be compared to that of the monomeric helicases such as RecQ and UvrD (reviewed in refs. 21,22). Here, the two ATPase domains create the driving force that pulls the continuous DNA strand through the protein, while a 'strand separation pin' splits the complementary strand from the template strand (Fig. 2j). In an analogous manner, in Pol I, the alternating opening of the O-helix and the addition of a new nucleotide into the growing primer strand act as the driving force for the continuous translocation of the template strand, while the fingers domain acts as the strand separation pin that splits the downstream primer from the template strand (Fig. 2k).

Pol I endonuclease and fingers domain compete for DNA binding

As Pol I performs strand displacement DNA synthesis it generates a single-stranded flap that becomes a substrate for the endonuclease domain. Yet how the endonuclease domain gains access to the single-stranded flap is not known. The 6-nt single-stranded flap in the displaced primer is not observed in the cryo-EM map, but based on the position of the visible 5′ end of the displaced primer the single-stranded flap would stand out on top of the fingers domain (Fig. 2c,d). Here it could be reached by the endonuclease domain that is connected to polymerase via a roughly 35 amino-acid unstructured linker (Fig. 3a). If fully stretched this linker could reach a distance of roughly 130 Å, which is further than the longest distance in the polymerase domain (80 Å). However, as mentioned above, in our structure of full-length Pol I no additional density was observed that can be attributed to the endonuclease domain, indicating that it is flexible in this structure, in agreement with the crystal structures of *Thermus aquaticus* Pol I (ref. 36) and that of *Mycobacterium smegmatis* Pol I (ref. 34) in which the endonuclease domain is found in two different positions (Extended Data Fig. 2b,c).

Fig. 2 | Cryo-EM structures of Pol I bound to an upstream and downstream DNA substrate. a, Front and top view of closed Pol I structure with different domains marked. The template DNA strand is marked in black, extended primer strand in green and displaced primer strand in red. **b**, Top view of the open Pol I structure. The fingers domain movement is marked by an orange arrow. The cartoon shows the movement of the DNA and O-helix compared to the closed structure. The unpaired base pair is marked by two short red lines. **c**, Schematic view of Pol I and DNA used for structure determination. Striped endonuclease domain indicates its absence in the structure. Sections of the DNA not observed in the cryo-EM map are shown as transparent. **d**, Close up of the displaced section of the DNA. Cryo-EM map is shown in gray mesh. Key DNA-interacting residues are shown in yellow sticks. **e**, Close up of the protein–DNA interactions of the displaced and extended DNA section. The pink arrow indicates the limited contact between the displaced DNA and fingers domain. Pink stars mark the contacts between the thumb domain and the extended section of DNA. **f**, Local resolution maps of the closed (left) and open (right) Pol I structures colored from high resolution (blue) to low resolution (red). Red dashes lines mark the position of the displaced and extended section of the DNA. **g**, Close up of the polymerase active site in the closed Pol I structure. Two aromatic residues that interact with the terminal base pair and the three glutamates and/or aspartates of the catalytic triad are shown with yellow sticks. **h**, The same view for the open Pol I structure. Movement of the DNA and the O-helix is marked with the two orange arrows. **i**, Electrostatic potential plot of the polymerase active site of the closed structure. A negatively charged patch (colored red) is located under the terminal 2 nts of the extended strand. Parts of thumb and fingers domain were omitted for clarity. **j**, Schematic drawing of strand displacement by monomeric helicases such as UvrD. **k**, The strand displacement by Pol I.

https://doi.org/10.1038/s41594-023-01071-y

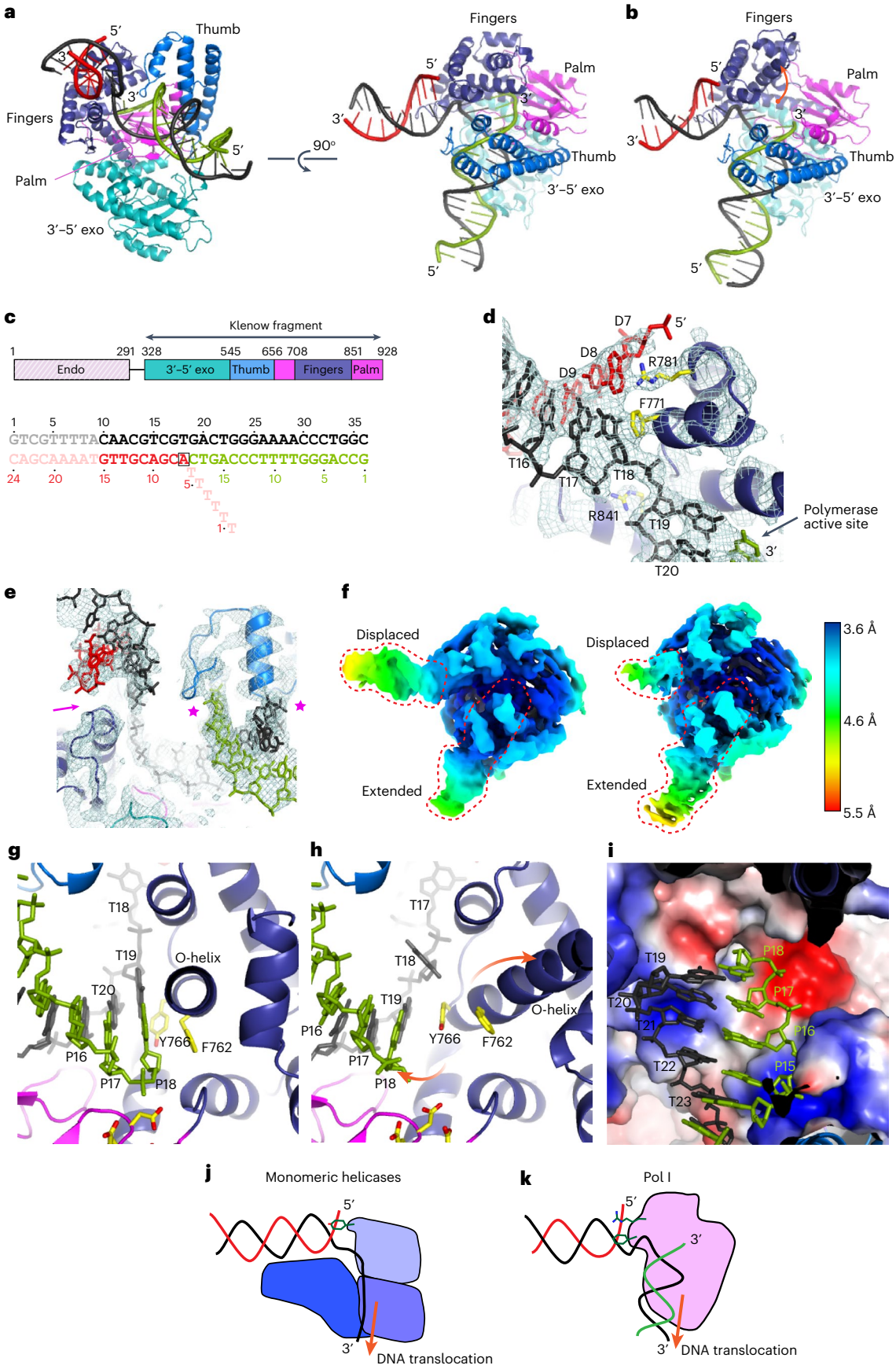

https://doi.org/10.1038/s41594-023-01071-y

Table 1 | Cryo-EM data collection, refinement and validation statistics

Data collection and processing	Pol I ^{FL}	Pol I ^{KL} open	Pol I ^{KL} closed
Magnification	105,000	105,000	105,000
Voltage (kV)	300	300	300
Electron exposure (e^-/Å^2)	54	50	50
Defocus range (μm)	0.8 to 2.0	0.8 to 2.0	0.8 to 2.0
Pixel size (Å)	0.836	0.836	0.836
Symmetry imposed	C1	C1	C1
Initial particle images (no)	800,892	565,078	565,078
Final particle images (no)	95,850	164,102	65,904
Map resolution (Å)	4.3	4.0	4.1
FSC threshold	0.143	0.143	0.143
Map resolution range (Å)	4.3 to roughly 10	4.0 to roughly 10	4.1 to roughly 10
Refinement			
Initial model used (PDB code)	1KLN	1KLN	1KLN
Model resolution (Å)	4.4	4.0	4.2
FSC threshold	0.5	0.5	0.5
Map sharpening *B* factor (Å^2)	−139		
Model composition			
Nonhydrogen atoms	5,864	5,829	5,891
Protein residues	603	604	604
DNA residues	53	51	54
***B* factors (Å^2)**			
Protein	52–162	32–148	73–186
DNA	64–263	54–275	81–254
R.m.s deviations			
Bond lengths (Å^2)	0.004	0.009	0.007
Bond angles (°)	1.164	1.059	0.831
Validation			
MolProbity score	1.81	1.94	1.97
Clashscore	6.56	12.84	14.32
Poor rotamers (%)	1.77	0	0
Ramachandran plot			
Favored (%)	96.17	95.35	95.51
Allowed (%)	3.83	4.65	4.15
Disallowed (%)	0	0	0.33

To gain insight into how the endonuclease domain might engage with the single-stranded flap, we used AlphaFold[37] to generate a model of the *E. coli* Pol I endonuclease domain that overlays well with the endonuclease domains of *T. aquaticus* and *M. smegmatis* Pol I (refs. 34,36) (Extended Data Fig. 2d). Next, as currently no structure has been determined for a Pol I endonuclease domain bound to DNA, we used DNA-bound structures of the structurally related FEN1 and T5 endonucleases[38,39] to model DNA binding (Extended Data Fig. 2e,f) and guide the endonuclease domain onto the displaced DNA section of our Pol I cryo-EM structure (Fig. 3b,c). The superimposition of the endonuclease domain results in a major clash with the fingers domain of the polymerase (Fig. 3d). This suggests that for the single-stranded flap to be cut by the endonuclease domain, the displaced section of the DNA may temporarily dissociate from the polymerase fingers domain. Indeed, biochemical and single molecule studies have shown that the endonuclease and polymerase domains alternate on the DNA[40,41]. However, this does not mean that the polymerase dissociates from the DNA completely as it can still hold on to the extended part of the DNA. This is also supported by the cryo-EM structure that shows that the extended section of the DNA is well defined in the cryo-EM map as it has numerous contacts with the protein, in contrast to the displaced section of the DNA that has only limited contact with the protein and is consequently less well defined in the cryo-EM map (Fig. 2e,f).

As the endonuclease and fingers domains compete for the same substrate, we wondered whether the action of the endonuclease domain can affect DNA synthesis by the polymerase domain. We compared three versions of Pol I: full-length Pol I, Pol I with the endonuclease domain deleted (Klenow fragment, Pol I^{KL}) and full-length Pol I in which two active site residues of the endonuclease domain (D115 and D140) were mutated to alanine to render it inactive (Pol I$^{endo\text{-}mut}$). On a DNA substrate without a downstream primer, all three proteins synthesize DNA in a similar manner, indicating that all versions retain full polymerase activity (Fig. 3e).

Also, in the presence of a downstream primer, both Pol I and Pol I^{KL} show a similar activity indicating that the endonuclease domain does not slow down the polymerase. By contrast, Pol I$^{endo\text{-}mut}$ shows a slowing down of polymerase activity with more intermediate fragments of the extended primer (Fig. 3f). This suggests that the mutated endonuclease binds to the displaced strand, but as it is not able to perform the incision, it remains bound to the displaced strand and slows down the polymerase. This supports the notion that the fingers domain and endonuclease domain alternate on the displaced section of the DNA, while the extended section of the DNA remains bound to the polymerase domain to continue DNA synthesis.

Finally, to determine whether the endonuclease requires a specific length of the single-stranded flap, we measured the endonuclease activity on a series of DNA substrates that mimic the progression of DNA strand displacement synthesis (Fig. 3g). Nucleotides were omitted to isolate the endonuclease activity from polymerase activity. On all the substrates, similar activity is observed, indicating that the endonuclease domain does not have a specific length requirement. While the endonuclease activity is distributive, on all substrates the predominant cut site is located 1 nt further than the end of the single-stranded flap, in agreement with earlier reports[17,18]. This is also consistent with our cryo-EM structures that show a 1 nt translation in the absence of nucleotides, thus enabling the endonuclease to cut one more nucleotide into the displaced strand. The data above indicate that while the displaced DNA section alternates from the polymerase fingers domain to the endonuclease domain, the extended DNA section remains attached to the polymerase domain (Fig. 3h). This also ensures that the displaced nucleotide in the template strand (nucleotide 18, Fig. 2h) remains bound in the polymerase active site and is prevented from re-annealing with the +1 unpaired nucleotide in the displaced strand that is therefore free to be excised by the endonuclease. It furthermore provides a possible explanation for the lack of density for the endonuclease domain as even when it engages with the single-strand DNA flap it remains flexible in the cryo-EM map as both the endonuclease domain and the displaced DNA section are now loosely tethered to the remainder of the polymerase.

Pol I endonuclease is an RNA–DNA-junction endonuclease

As all experiments above were conducted with a DNA downstream primer, we also compared the endonuclease incision on an RNA–DNA-hybrid downstream primer that is similar to the natural substrate encountered during Okazaki maturation (Fig. 4a). In the absence of dNTPs, when the polymerase cannot proceed, we find that the endonuclease removes the first 1 or 2 nt on both the DNA and RNA–DNA substrate (Fig. 4a). We also find that on the RNA–DNA substrate an additional incision takes place at the junction between the RNA and DNA.

https://doi.org/10.1038/s41594-023-01071-y

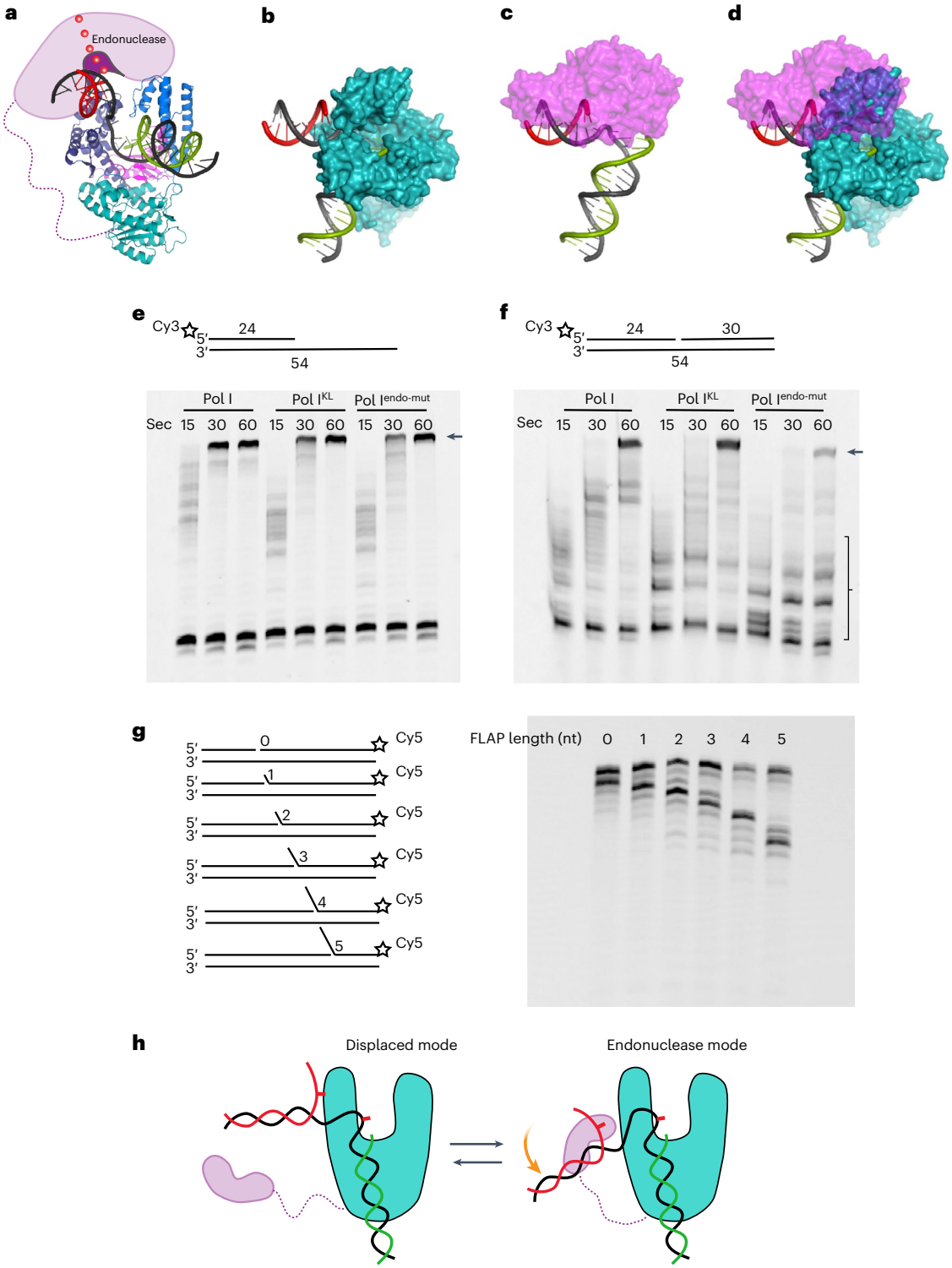

Fig. 3 | Alternating activities of polymerase fingers and endonuclease domains. a, The front view of the Pol I-DNA structure with the predicted position of endonuclease domain marked out with the pinky-purple cartoon. The approximate position of the single-stranded flap is indicated by the red spheres. **b**, Cryo-EM structure of Pol I bound to an Okazaki fragment. Pol I is shown in blue surface, the template strand in black, the extended primer in green and displaced primer in red. View similar to Fig. 2a,b. **c**, Model of Pol I endonuclease domain bound to the displaced primer. Endonuclease domain shown in transparent magenta surface. For modeling details, see Extended Data Fig. 2. **d**, Combined structures of Pol I and endonuclease domain reveal a large overlap between the two structures. **e**, Primer extension activity on a primed substrate by Pol I, Pol I Klenow fragment (Pol I^{KL}) and Pol I with inactive endonuclease domain (Pol I$^{endo\text{-}mut}$). The arrow marks the full-length product. **f**, Primer extension activity on a double primed substrate. The arrow marks full-length product and bracket marks incomplete products. **g**, Endonuclease activity of Pol I on DNA substrates with different lengths of single-stranded flaps (0–5 nt). For all reactions, 100 nM protein and 100 nM DNA substrate was used. **h**, A cartoon model showing a possible movement of the displaced DNA section from the polymerase fingers domain to the endonuclease domain during the displaced and endonuclease modes, respectively. The model shows the open Pol I structure in which the DNA has translated by one nucleotide and the first base pair of the displaced DNA sections has been unpaired. The polymerase domain (Klenow fragment) is shown in cyan, endonuclease domain in pinky-purple, continuous template strand in black, extended strand in green and displaced strand in red. The unpaired base pair is shown in red.

https://doi.org/10.1038/s41594-023-01071-y

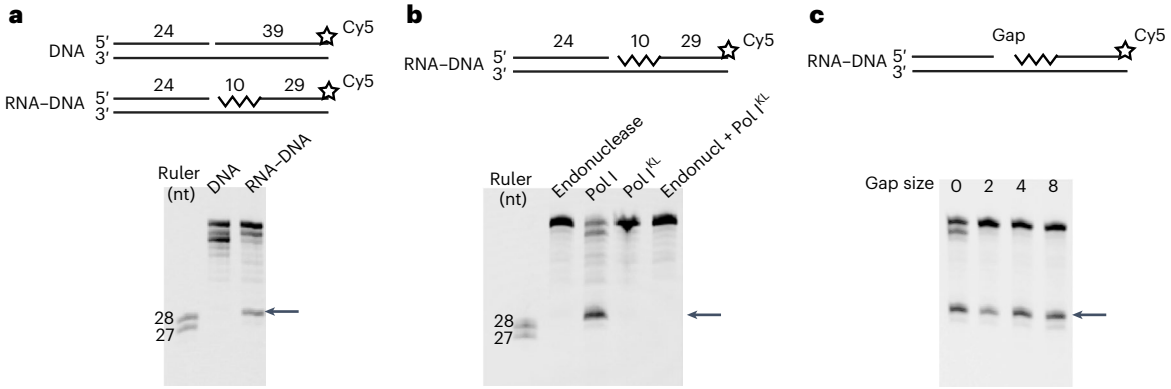

Fig. 4 | Pol I endonuclease cuts at the RNA–DNA junction. a, Endonuclease activity of Pol I on an all DNA downstream primer ('DNA') and an RNA–DNA downstream primer ('RNA–DNA') containing ten RNA nts (indicated by the zig-zag line) and 29 DNA nts. The arrow marks the 29 nt product after incision at the RNA–DNA junction. **b**, Endonuclease activity on the RNA–DNA substrate of the isolated endonuclease domain, full-length Pol I, the isolated Pol I^{KL} domain and the isolated endonuclease domain in combination with the Pol I^{KL} domain. **c**, Endonuclease activity on RNA–DNA substrate with an increasing gap size between the upstream primer and downstream primer. For all reactions, 100 nM protein and 100 nM DNA substrate were used.

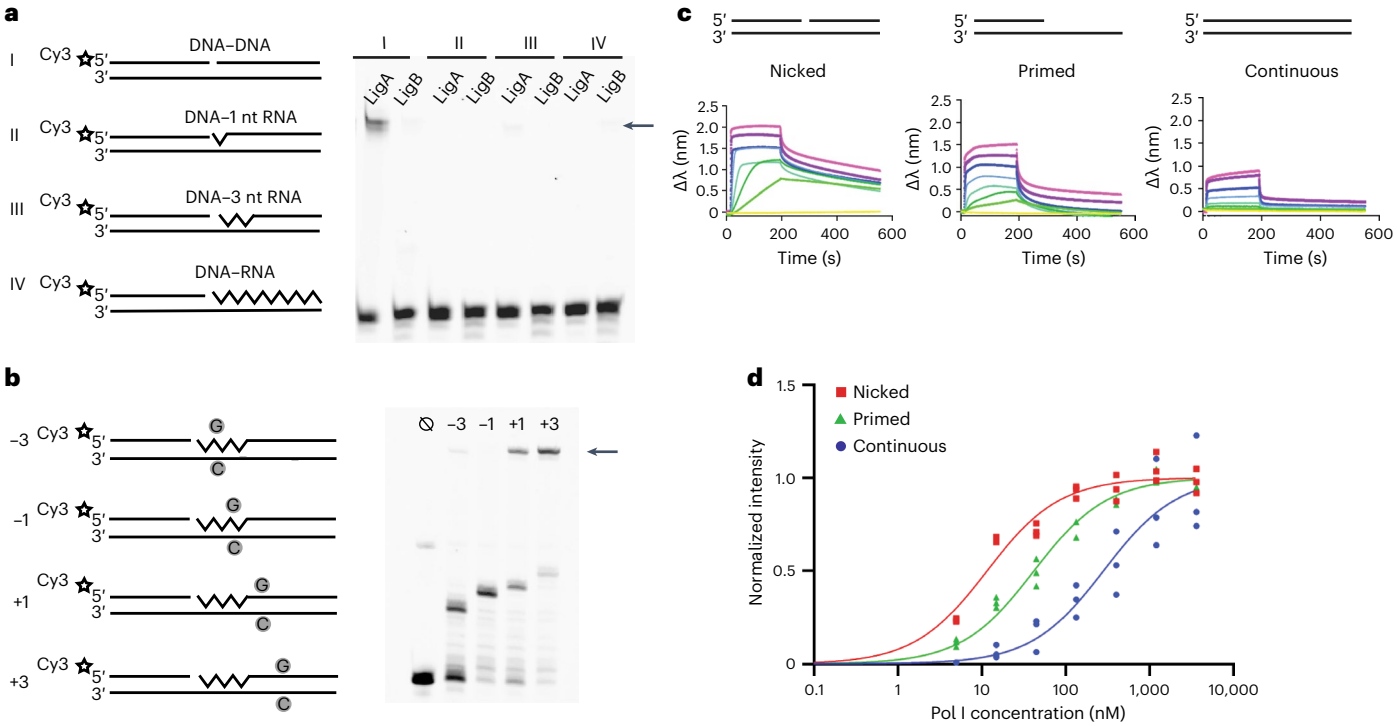

Fig. 5 | Ligase activity of the *E. coli* LigA and LigB. a, The left panel shows different DNA–DNA and DNA–RNA substrates used for the ligation assay. The right panel shows ligase activity of LigA and LigB on the different DNA–RNA substrates. The arrow marks the full-length ligated product. **b**, The left panel shows DNA–RNA substrates with defined stop sites in the RNA and DNA section of the downstream primer. Stop sites are marked with 'G' and 'C' in a gray circle. The right panel shows primer extension and ligation activity of Pol I and LigA on the different DNA–RNA substrates with defined stop sites. The arrow marks the full-length ligated product. For all reactions, 100 nM protein and 100 nM DNA substrate were used. **c**, Bio-layer interferometry association and dissociation curves of Pol I on three DNA substrates: a nicked substrate with both an extended and displaced primer, a primed substrate with only an extended primer and a continuous substrate with both template and primer strand of equal length. Different colors indicate increasing protein concentration. Δλ indicates the color shift in the measured light. Pol I concentration ranging from 0.05 to 3.6 μM. **d**, DNA binding curves of Pol I to the three DNA substrates derived from the bio-layer interferometry curves. Data points mark the value at $t = 180$ when association has saturated. Red squares indicate nicked DNA, green triangles primed DNA and blue circles continuous DNA. Data points are derived from three independent experiments and are normalized to the maximum binding value. Derived K_d values for the different DNA substrates are: nicked 12 ± 5 nM, primed 80 ± 8 nM and continuous 800 ± 10 nM.

The structurally unrelated type 2 RNases H are also RNA–DNA-junction directed endonucleases but these cut the RNA primer 1 nt before the RNA–DNA junction[42,43] and not at the junction as the Pol I endonuclease domain.

The RNA–DNA-junction directed endonuclease activity is not observed for the isolated endonuclease domain, nor when polymerase and endonuclease domains are added as separate proteins (Fig. 4b) suggesting that polymerase domain and endonuclease work together. The RNA–DNA-junction specific incision is also observed on substrates with an increasing gap between the extended primer and the downstream primer where the polymerase is positioned further away from the downstream primer (Fig. 4c). This suggests that the requirement of the

https://doi.org/10.1038/s41594-023-01071-y

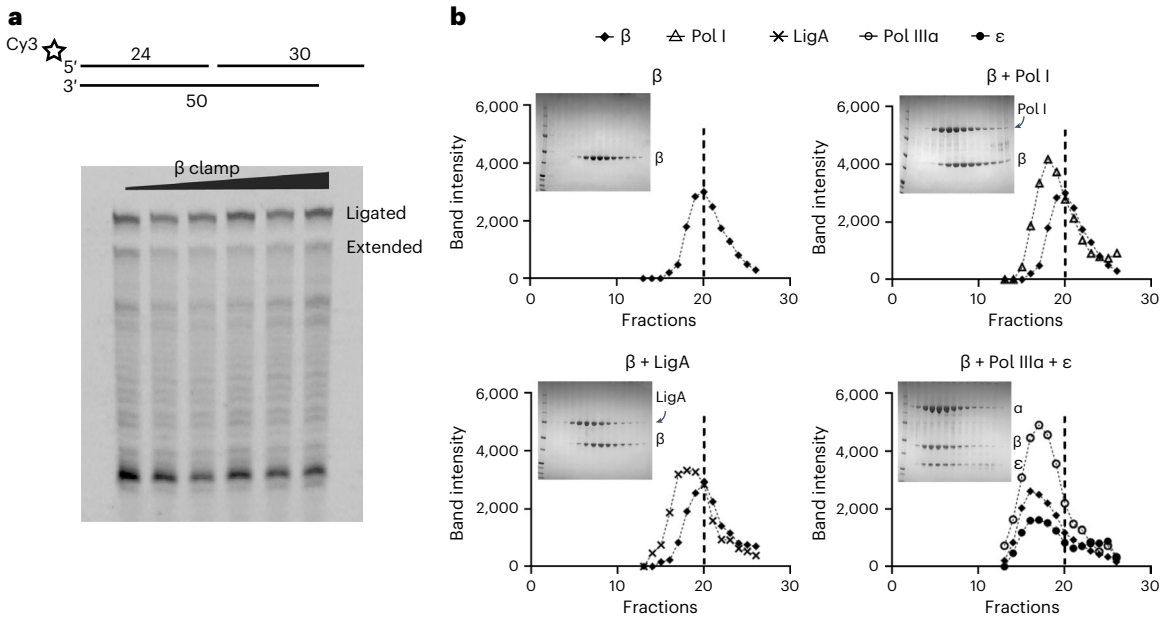

Fig. 6 | The β clamp does not appear to play a role in Okazaki fragment maturation. a, The top shows the DNA substrate used for primer extension assay. The displaced primer is 4 nt longer than the template strand so that the ligated product can be separated from the extended product that will be of the same size as the template strand. The bottom shows the primer extension assay performed with increasing amounts of β clamp (0–1.8 μM) and 100 nM Pol I and LigA and 100 nM DNA substrate. **b**, Analytical size exclusion chromatography of β clamp in the presence of Pol I, LigA and Pol IIIαε. All proteins were injected at 10 μM. Fractions of the chromatography run were analyzed by SDS–PAGE (inserts) and protein band intensities quantified. Graphs show intensities of the individuals protein bands, plotted by fraction number. The dashed vertical line indicates the peak for the isolated β clamp at fraction 20.

polymerase domain is mainly to bring the endonuclease to the RNA–DNA substrate, rather than directly affect the downstream RNA–DNA primer. The incision at the RNA–DNA junction is intriguing as it may make the removal of the RNA primer more efficient. By marking the end of the RNA primer it could help prevent the continuation of the strand displacement into the DNA section of the downstream primer. Finally, given that the RNA–DNA junction is structurally different from the single-stranded flap that is also cut by the Pol I endonuclease, it seems likely that a different mechanism might be at work for this substrate, but how Pol I endonuclease recognizes and cuts an RNA–DNA junction remains to be determined.

LigA seals the nick when the RNA is completely removed

When Pol IIIα terminates DNA synthesis at the downstream primer it leaves a nick that can be ligated when the downstream primer is DNA (Fig. 1c). However, during replication, each segment is preceded by an RNA primer that contains a triphosphate tail at its 5′ end[7] that is not a compatible substrate for ligase activity[27]. However, the flap-directed action of the endonuclease does create clean 5′ ends that could potentially become a target for a ligase.

Therefore, to determine whether the ligation can occur at a DNA–RNA junction, we tested the two *E. coli* ligases, LigA and LigB, on a series of downstream primers with different number of RNA nucleotides (Fig. 5a). On a DNA–DNA substrate, LigA, but not LigB, efficiently ligates the two primers, in agreement with earlier reports[44]. No ligase activity by either LigA or LigB is observed on any of the RNA downstream primers in agreement with early work[45].

Thus, the lack of ligase activity on a DNA–RNA junction prevents the incorporation of RNA into the DNA. However, this raises the question: how is Pol I prevented from continuing strand displacement synthesis too far into the DNA section past the RNA primer? We therefore wondered whether there may be a role for LigA to evict the polymerase from DNA once the RNA primer has been removed. We designed a series of RNA–DNA substrates that contain a single C in the template strand. By omitting the complementary dGTP from the nucleotide mix during the polymerase assay, we create stop sites that Pol I cannot bypass (Extended Data Fig. 3). The stop positions were chosen at two sites in the RNA primer, at −3 or −1 nts from the RNA–DNA junction, and at two sites in the DNA primer, at +1 or +3 from the RNA–DNA junction (Fig. 5b). All reactions were performed in the presence of LigA, Pol I and the three nucleotides dATP, dCTP and dTTP. On both substrates where the single C is placed in the RNA section, we find that the polymerase comes to a halt and the downstream primer is not ligated to the extended primer as LigA cannot ligate DNA to RNA (Fig. 5a). By contrast, when the single C is located in the DNA section, we also observe a pause of the polymerase, but the remaining product is now ligated to the extended primer to produce a full-length primer strand. Hence, only when the polymerase reaches the DNA section LigA can close the nick.

Next, to determine how the ligation of a nicked substrate impacts the binding of the polymerase, we used bio-layer interferometry to measure the affinity of Pol I for three DNA substrates: a primed, a nicked and a continuous DNA substrate (Fig. 5c,d). To prevent end-binding by the polymerase, the free ends of the DNA substrates were blocked by streptavidin. The polymerase binds with high affinity to a nicked substrate ($K_d = 12 \pm 5$ nM), with a 3.5-fold lower affinity for a primed substrate ($K_d = 42 \pm 5$ nM) and a 24-fold lower affinity for a continuous stretch of DNA ($K_d = 285 \pm 5$ nM) (Fig. 5d), indicating that as soon as the nick is sealed by LigA, the polymerase will no longer be able to engage with the DNA. Hence, LigA plays a crucial role in discriminating between the RNA and DNA section of the downstream primer and the release of Pol I from the DNA. In combination with the RNA–DNA-junction specific incision of the endonuclease at the end of the RNA primer, it makes for an efficient removal of the RNA primer and prevents the continuation of the strand displacement into the DNA section.

The β clamp has a limited role in RNA primer removal

The β clamp is essential during DNA replication, where it binds to Pol IIIαε and greatly enhances its processivity[10,11]. When Pol IIIα terminates synthesis on a downstream RNA primer and dissociates, the clamp remains bound to the DNA[26,46,47] and becomes available for

Pol I and LigA to bind to. However, contrasting reports exist about the role of the β clamp during Okazaki fragment maturation. While early reports show a stimulating effect of the β clamp on the polymerase activity of Pol I (ref. 48), more recent work shows a negative effect[49]. Similarly, early work indicates an interaction between the *E. coli* ligase and β clamp[48], while more recently it was reported that the *Mycobacterium tuberculosis* ligase and the β clamp do not interact[50]. This contrasts with the eukaryotic system, where the three proteins Pol δ, FEN1 and ligase depend on the eukaryotic clamp PCNA[51–54]. Therefore, to determine whether the β clamp influences Okazaki fragment maturation, we designed a DNA substrate that can discriminate between polymerase and ligase activity by using a downstream primer that is longer than the template strand (Fig. 6a). As a result, ligation will give a longer product than primer extension by the polymerase. It is important to note that on a similar open ended DNA substrate the β clamp can load itself onto the DNA without the use of the clamp loader complex[55] and form a complex with Pol IIIαε on DNA[56,57]. Next, using increasing amounts of the β clamp we do not observe a change in the ratio between the extended or the ligated product, indicating that the β clamp does not affect the activity of the two proteins. Following this, we also analyzed the direct interaction between the β clamp and Pol I or LigA by size exclusion chromatography followed by SDS–PAGE. As judged by the measured SDS–PAGE band intensity of the protein of the elution peak shown in Fig. 6b, the migration of the β clamp is unaltered by the presence of Pol I or LigA. By contrast, we find a clear shift in the retention volume of the β clamp in the presence of Pol IIIαε that together firmly bind to the clamp[56,58]. Finally, when mapping the predicted β-binding motifs on Pol I and LigA, we find that they are located in regions of the proteins that are not accessible to the clamp (Extended Data Fig. 4). Taken together, our data indicate that the β clamp does not play a role in Okazaki fragment maturation in *E. coli*.

Discussion

During DNA replication, thousands of RNA primers are incorporated into the lagging strand that subsequently need to be removed. This is achieved by a series of proteins that remove the RNA primer, resynthesize the DNA and ligate two adjacent Okazaki fragments. To ensure that this process is performed efficiently, it is essential that the process is well orchestrated. Here, we show that each protein acts as a team member in a molecular relay race, where each protein prepares the DNA–RNA substrate for the next protein to act on (Fig. 7). (1) Pol IIIαε synthesizes DNA all the way up to the RNA primer, leaving only a nick. (2) As LigA cannot ligate a DNA–RNA junction, Pol I continues DNA synthesis while displacing the RNA primer that becomes a target for the Pol I endonuclease domain. (3) The Pol I endonuclease domain also specifically nicks the downstream primer at the RNA–DNA junction to mark the end of the RNA primer. (4) Once all of the RNA primer has been removed, LigA will ligate the nick, preventing further association of the polymerase and leaving an intact DNA fragment. This way, the activities of Pol IIIαε, Pol I polymerase, Pol I endonuclease and LigA act as a four-point molecular relay race in which each activity is well-coordinated to ensure a fast and efficient removal of the thousands of RNA primers incorporated into the lagging strand during DNA synthesis.

Eukaryotic DNA replication also uses RNA primers that are removed from the lagging strand after DNA replication, albeit using a slightly different approach. The lagging strand DNA polymerase δ itself contains modest strand displacement properties[59–61], while the leading strand polymerase Pol ε does not[59,62]. Yet, unlike Pol I that can displace large stretches of RNA or DNA, Pol δ can only displace 1–2 nt after which its 3′–5′ proofreading exonuclease will resect the newly synthesized nucleotides, resulting in 'idling' of the polymerase at the nick[61,63]. Therefore, the action of Flap endonuclease 1 (FEN1) is required to remove the displaced flap and allow Pol δ to continue its strand displacement synthesis[9,64]. FEN1 distinguishes itself from the bacterial

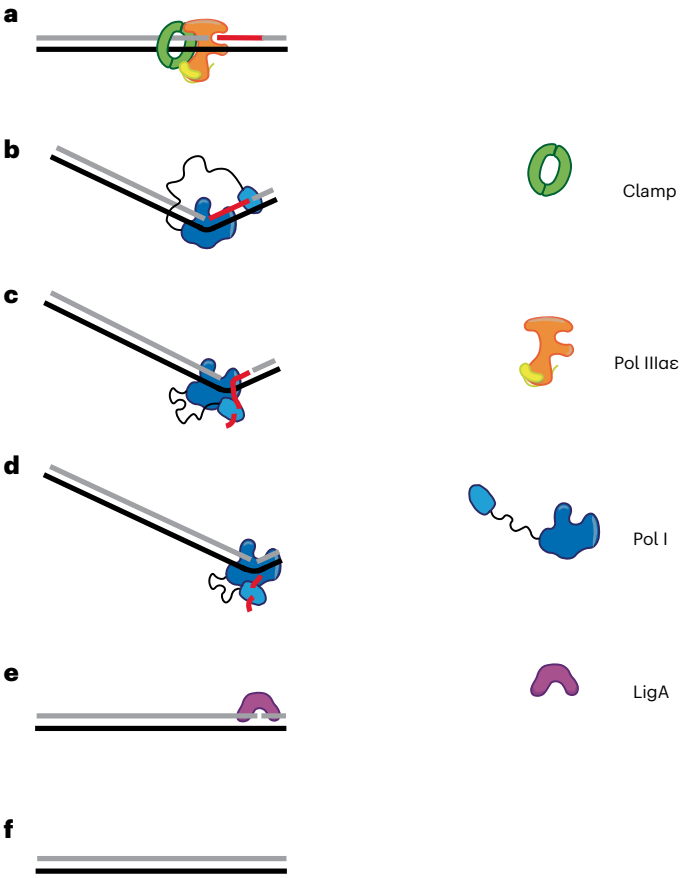

Fig. 7 | Schematic representation of Okazaki fragment maturation. a, The replicative polymerase Pol IIIα, bound to the β clamp and ε exonuclease will synthesize up to the last nucleotide before the RNA primer where it will fall off. **b**, Pol I will then bind to the DNA–RNA substrate and kink the DNA to facilitate strand displacement DNA synthesis. In addition, the endonuclease domain will incise the downstream primer at the RNA–DNA junction and mark the end of the RNA primer. **c**, Pol I will then extend the newly synthesized strand, while at the same time displacing the downstream RNA primer. **d**, The displaced strand is cleaved by the endonuclease domain until all of the RNA primer has been removed. **e**, The DNA–DNA junction becomes a substrate for the DNA ligase LigA that will close the gap. **f**, This leaves a continuous DNA strand.

endonuclease in two ways: FEN1 is an isolated protein that requires the interaction with the DNA sliding clamp PCNA for optimal activity[53] and only cuts short 1–2 nt flaps[61,65]. Like the bacterial system, the process is finalized by the sealing of the nick by a DNA ligase LIG1. LIG1, such as the *E. coli* LigA, will only ligate DNA to DNA[27] and therefore prevent incorporation of the RNA primer into the continuous DNA strand. Unlike *E. coli* LigA, however, LIG1 relies on the eukaryotic sliding clamp PCNA for its activity[51]. In addition, once LIG1 has sealed the nick, it remains bound to the DNA and PCNA[66], although the reason for this remains unclear.

Finally, the highly processive strand displacement DNA synthesis of Pol I is the basis for loop mediated isothermal amplification (LAMP) that is used for rapid detection of DNA[67]. In combination with reverse transcriptase, the same approach can be used for the amplification of RNA, as used for the detection of SARS-CoV-2 virus[68,69]. Due to the isothermal reaction conditions, LAMP reactions can deliver positive results in under 10 minutes (ref. 70), compared to 3 hours for traditional PCR-based detection methods[71]. The isothermal reaction condition furthermore removes the requirement for specialized equipment, making it possible to use it in remote places and less-developed areas of the world[72]. Our structure of Pol I engaged with both the extended and displaced primer will be of value to further the developments of the

enzymes used in the LAMP reaction to shorten reaction times, increase sensitivity and accuracy and create a fast, sensitive and reliable assay that can be used all over the world.

Online content

Any methods, additional references, Nature Portfolio reporting summaries, source data, extended data, supplementary information, acknowledgements, peer review information; details of author contributions and competing interests; and statements of data and code availability are available at https://doi.org/10.1038/s41594-023-01071-y.

References

1. Mok, M. & Marians, K. J. The *Escherichia coli* preprimosome and DNA B helicase can form replication forks that move at the same rate. *J. Biol. Chem.* **262**, 16644–16654 (1987).
2. McInerney, P., Johnson, A., Katz, F. & O'Donnell, M. Characterization of a triple DNA polymerase replisome. *Mol. Cell* **27**, 527–538 (2007).
3. Yao, N. Y., Georgescu, R. E., Finkelstein, J. & O'Donnell, M. E. Single-molecule analysis reveals that the lagging strand increases replisome processivity but slows replication fork progression. *Proc. Natl Acad. Sci. USA* **106**, 13236–13241 (2009).
4. Sakabe, K. & Okazaki, R. A unique property of the replicating region of chromosomal DNA. *Biochim. Biophys. Acta.* **129**, 651–654 (1966).
5. Okazaki, R. Mechanism of DNA chain growth. *J. Mol. Biol.* **95**, 63–70 (1967).
6. Blattner, F. R. et al. The complete genome sequence of *Escherichia coli* K-12. *Science* **277**, 1453–1462 (1997).
7. Kitani, T., Yoda, K. Y., Ogawa, T. & Okazaki, T. Evidence that discontinuous DNA replication in *Escherichia coli* is primed by approximately 10 to 12 residues of RNA starting with a purine. *J. Mol. Biol.* **184**, 45–52 (1985).
8. Wu, C. A., Zechner, E. L., Reems, J. A., McHenry, C. S. & Marians, K. J. Coordinated leading- and lagging-strand synthesis at the *Escherichia coli* DNA replication fork. V. Primase action regulates the cycle of Okazaki fragment synthesis. *J. Biol. Chem.* **267**, 4074–4083 (1992).
9. Balakrishnan, L. & Bambara, R. A. Okazaki fragment metabolism. *Cold Spring Harb. Perspect. Biol.* **5**, a010173 (2013).
10. LaDuca, R. J., Crute, J. J., McHenry, C. S. & Bambara, R. A. The β subunit of the *Escherichia coli* DNA polymerase III holoenzyme interacts functionally with the catalytic core in the absence of other subunits. *J. Biol. Chem.* **261**, 7550–7557 (1986).
11. Stukenberg, P. T., Studwell-Vaughan, P. S. & O'Donnell, M. Mechanism of the sliding β-clamp of DNA polymerase III holoenzyme. *J. Biol. Chem.* **266**, 11328–11334 (1991).
12. Georgescu, R. E. et al. Mechanism of polymerase collision release from sliding clamps on the lagging strand. *EMBO J.* **28**, 2981–2991 (2009).
13. Lundquist, R. C. & Olivera, B. M. Transient generation of displaced single-stranded DNA during nick translation. *Cell* **31**, 53–60 (1982).
14. Singh, K., Srivastava, A., Patel, S. S. & Modak, M. J. Participation of the fingers subdomain of *Escherichia coli* DNA polymerase I in the strand displacement synthesis of DNA. *J. Biol. Chem.* **282**, 10594–10604 (2007).
15. Klett, R. P., Cerami, A. & Reich, E. Exonuclease VI, a new nuclease activity associated with *E. coli* DNA polymerase. *Proc. Natl Acad. Sci. USA* **60**, 943–950 (1968).
16. Kelly, R. B. Enzymatic synthesis of deoxyribonucleic acid. *J. Biol. Chem.* **53**, 83–112 (1970).
17. Lyamichev, V., Brow, M. A. D. & Dahlberg, J. E. Structure-specific endonucleolytic cleavage of nucleic acids by eubacterial DNA polymerases. *Science* **260**, 778–783 (1993).
18. Xu, Y. et al. Biochemical and mutational studies of the 5′-3′ exonuclease of DNA polymerase I of *Escherichia coli*. *J. Mol. Biol.* **268**, 284–302 (1997).
19. Sugimoto, K., Okazaki, T. & Okazaki, R. Mechanism of DNA chain growth, II. Accumulation of newly synthesized short chains in *E. coli* infected with ligase-defective T4 phages. *Proc. Natl Acad. Sci. USA* **60**, 1356–1362 (1968).
20. Pauling, C. & Hamm, L. Properties of a temperature-sensitive, radiation-sensitive mutant of *Escherichia coli*. II. DNA replication. *Proc. Natl Acad. Sci. USA* **64**, 1195–1202 (1969).
21. Gao, Y. & Yang, W. Different mechanisms for translocation by monomeric and hexameric helicases. *Curr. Opin. Struct. Biol.* **61**, 25–32 (2020).
22. Meir, A. & Greene, E. C. Srs2 and pif1 as model systems for understanding sf1a and sf1b helicase structure and function. *Genes (Basel)* **12**, 1319 (2021).
23. Yuan, Q. & McHenry, C. S. Strand displacement by DNA polymerase III occurs through a τ-ψ-χ link to single-stranded DNA-binding protein coating the lagging strand template. *J. Biol. Chem.* **284**, 31672–31679 (2009).
24. Schwartz, J. J. & Quake, S. R. Single molecule measurement of the 'speed limit' of DNA polymerase. *Proc. Natl Acad. Sci. USA* **106**, 20294–20299 (2009).
25. O'Donnell, M. E. & Kornberg, A. Complete replication of templates by *Escherichia coli* DNA polymerase III holoenzyme. *J. Biol. Chem.* **260**, 12884–12889 (1985).
26. Leu, F. P., Georgescu, R. & O'Donnell, M. Mechanism of the *E. coli* τ processivity switch during lagging-strand synthesis. *Mol. Cell* **11**, 315–327 (2003).
27. Pascal, J. M. DNA and RNA ligases: structural variations and shared mechanisms. *Curr. Opin. Struct. Biol.* **18**, 96–105 (2008).
28. Johnson, K. A. The kinetic and chemical mechanism of high-fidelity DNA polymerases. *Biochim. Biophys. Acta - Proteins Proteom.* **1804**, 1041–1048 (2010).
29. Santoso, Y. et al. Conformational transitions in DNA polymerase I revealed by single-molecule FRET. *Proc. Natl Acad. Sci. USA* **107**, 715–720 (2010).
30. Miller, B. R., Beese, L. S., Parish, C. A. & Wu, E. Y. The closing mechanism of DNA polymerase I at atomic resolution. *Structure* **23**, 1609–1620 (2015).
31. Beese, L. S., Derbyshire, V. & Steitz, T. A. Structure of DNA polymerase I Klenow fragment bound to duplex DNA. *Science* https://doi.org/10.1142/9789811215865_0028 (1993).
32. Eom, S. H., Wang, J. & Steitz, T. A. Structure of Taq polymerase with DNA at the polymerase active site. *Nature* **382**, 293–296 (1996).
33. Kiefer, J. R., Mao, C. & Beese, L. S. Visualizing DNA replication in a catalytically active *Bacillus* DNA polymerase crystal. *Nature* **391**, 304–307 (1998).
34. Ghosh, S., Goldgur, Y. & Shuman, S. Mycobacterial DNA polymerase I: activities and crystal structures of the POL domain as apoenzyme and in complex with a DNA primer-template and of the full-length FEN/EXO–POL enzyme. *Nucleic Acids Res.* **48**, 3165–3180 (2020).
35. Craggs, T. D. et al. Substrate conformational dynamics facilitate structure-specific recognition of gapped DNA by DNA polymerase. *Nucleic Acids Res.* **47**, 10788–10800 (2019).
36. Kim, Y. et al. Crystal structure of *Thermus aquaticus* DNA polymerase. *Nature* **376**, 288–292 (1995).
37. Jumper, J. et al. Highly accurate protein structure prediction with AlphaFold. *Nature* **596**, 583–589 (2021).
38. AlMalki, F. A. et al. Direct observation of DNA threading in flap endonuclease complexes. *Nat. Struct. Mol. Biol.* **23**, 640–646 (2016).
39. Tsutakawa, S. E. et al. Phosphate steering by Flap Endonuclease 1 promotes 5′-flap specificity and incision to prevent genome instability. *Nat. Commun.* **8**, 15855 (2017).

40. Xu, Y., Grindley, N. D. F. & Joyce, C. M. Coordination between the polymerase and 5′-nuclease components of DNA polymerase I of *Escherichia coli*. *J. Biol. Chem.* **275**, 20949–20955 (2000).
41. Pauszek, R. F. III, Lamichhane, R., Singh, A. R. & Millar, D. P. Single-molecule view of coordination in a multi-functional DNA polymerase. *eLife* **10**, e62046 (2021).
42. Ohtani, N., Tomita, M. & Itaya, M. Junction ribonuclease: a ribonuclease HII orthologue from *Thermus thermophilus* HB8 prefers the RNA-DNA junction to the RNA/DNA heteroduplex. *Biochem. J.* **412**, 517–526 (2008).
43. Rychlik, M. P. et al. Crystal structures of RNase H2 in complex with nucleic acid reveal the mechanism of RNA-DNA junction recognition and cleavage. *Mol. Cell* **40**, 658–670 (2010).
44. Sriskanda, V. A second NAD^+-dependent DNA ligase (LigB) in *Escherichia coli*. *Nucleic Acids Res.* **29**, 4930–4934 (2001).
45. Olivera, B. M. Enzymic joining of polynucleotides. *J. Mol. Biol.* **46**, 481–492 (1968).
46. Stukenberg, P. T., Turner, J. & O'Donnell, M. An explanation for lagging strand replication: polymerase hopping among DNA sliding clamps. *Cell* **78**, 877–887 (1994).
47. López De Saro, F. J., Georgescu, R. E., Goodman, M. F. & O'Donnell, M. Competitive processivity-clamp usage by DNA polymerases during DNA replication and repair. *EMBO J.* **22**, 6408–6418 (2003).
48. López de Saro, F. J. & O'Donnell, M. Interaction of the β sliding clamp with MutS, ligase, and DNA polymerase I. *Proc. Natl Acad. Sci. USA* **98**, 8376–8380 (2001).
49. Bhardwaj, A., Ghose, D., Gopal Thakur, K. & Dutta, D. *Escherichia coli* β-clamp slows down DNA polymerase I dependent nick translation while accelerating ligation. *PLoS ONE* **13**, e0199559 (2018).
50. Kukshal, V. et al. *M. tuberculosis* sliding β-clamp does not interact directly with the NAD^+-dependent DNA ligase. *PLoS ONE* **7**, e35702 (2012).
51. Levin, D. S., Bai, W., Yao, N., O'Donnell, M. & Tomkinson, A. E. An interaction between DNA ligase I and proliferating cell nuclear antigen: implications for Okazaki fragment synthesis and joining. *Proc. Natl Acad. Sci. USA* **94**, 12863–12868 (1997).
52. Zhang, P. et al. Direct interaction of proliferating cell nuclear antigen with the p125 catalytic subunit of mammalian DNA polymerase δ. *J. Biol. Chem.* **274**, 26647–26653 (1999).
53. Gomes, X. V. & Burgers, P. M. J. Two modes of FEN1 binding to PCNA regulated by DNA. *EMBO J.* **19**, 3811–3821 (2000).
54. Xie, B. et al. Reconstitution and characterization of the human DNA polymerase delta four-subunit holoenzyme. *Biochemistry* **41**, 13133–13142 (2002).
55. Georgescu, R. E. et al. Structure of a sliding clamp on DNA. *Cell* **132**, 43–54 (2008).
56. Fernandez-Leiro, R., Conrad, J., Scheres, S. H. W. & Lamers, M. H. cryo-EM structures of the *E. coli* replicative DNA polymerase reveal its dynamic interactions with the DNA sliding clamp, exonuclease and τ. *eLife* https://doi.org/10.7554/eLife.11134 (2015).
57. Fernandez-Leiro, R. et al. Self-correcting mismatches during high-fidelity DNA replication. *Nat. Struct. Mol. Biol.* **24**, 140–143 (2017).
58. Toste Rêgo, A., Holding, A. N., Kent, H. & Lamers, M. H. Architecture of the Pol III-clamp-exonuclease complex reveals key roles of the exonuclease subunit in processive DNA synthesis and repair. *EMBO J.* **32**, 1334–1343 (2013).
59. Garg, P., Stith, C. M., Sabouri, N., Johansson, E. & Burgers, P. M. Idling by DNA polymerase δ maintains a ligatable nick during lagging-strand DNA replication. *Genes Dev.* **18**, 2764–2773 (2004).
60. Rossi, M. L., Purohit, V., Brandt, P. D. & Bambara, R. A. Lagging strand replication proteins in genome stability and DNA repair. *Chem. Rev.* **106**, 453–473 (2006).
61. Stodola, J. L. & Burgers, P. M. Resolving individual steps of Okazaki-fragment maturation at a millisecond timescale. *Nat. Struct. Mol. Biol.* **23**, 402–408 (2016).
62. Ganai, R. A. & Johansson, E. DNA replication—a matter of fidelity. *Mol. Cell* **62**, 745–755 (2016).
63. Jin, Y. H. et al. The 3′→5′ exonuclease of DNA polymerase δ can substitute for the 5′ flap endonuclease Rad27/Fen1 in processing Okazaki fragments and preventing genome instability. *Proc. Natl Acad. Sci. USA* **98**, 5122–5127 (2001).
64. Grasby, J. A., Finger, L. D., Tsutakawa, S. E., Atack, J. M. & Tainer, J. A. Unpairing and gating: sequence-independent substrate recognition by FEN superfamily nucleases. *Trends Biochem. Sci.* **37**, 74–84 (2012).
65. Stith, C. M., Sterling, J., Resnick, M. A., Gordenin, D. A. & Burgers, P. M. Flexibility of eukaryotic Okazaki fragment maturation through regulated strand displacement synthesis. *J. Biol. Chem.* **283**, 34129–34140 (2008).
66. Matsumoto, Y., Brooks, R. C., Sverzhinsky, A., Pascal, J. M. & Tomkinson, A. E. Dynamic DNA-bound PCNA complexes co-ordinate Okazaki fragment synthesis, processing and ligation. *J. Mol. Biol.* **432**, 166698 (2020).
67. Notomi, T. et al. Loop-mediated isothermal amplification of DNA. *Nucleic Acids Res.* **28**, E63 (2000).
68. Thompson, D. & Lei, Y. Mini review: recent progress in RT-LAMP enabled COVID-19 detection. *Sens. Actuators Rep.* **2**, 100017 (2020).
69. Kashir, J. & Yaqinuddin, A. Loop mediated isothermal amplification (LAMP) assays as a rapid diagnostic for COVID-19. *Med. Hypotheses* **141**, 109786 (2020).
70. Mautner, L. et al. Rapid point-of-care detection of SARS-CoV-2 using reverse transcription loop-mediated isothermal amplification (RT-LAMP). *Virol. J.* **17**, 160 (2020).
71. Mackay, I. M., Arden, K. E. & Nitsche, A. Real-time PCR in virology. *Nucleic Acids Res.* **30**, 1292–1305 (2002).
72. Rabe, B. A. & Cepko, C. SARS-CoV-2 detection using isothermal amplification and a rapid, inexpensive protocol for sample inactivation and purification. *Proc. Natl Acad. Sci. USA* **117**, 24450–24458 (2020).